Super-resolution Photoacoustic Microscopy Using a Localized Near-field of a Plasmonic Nanoaperture: A Three-dimensional Simulation Study

Byullee Park[1], Hongki Lee[2], Paul Kumar Upputuri[3], Manojit Pramanik[3*], Donghyun Kim[2*], and Chulhong Kim[1*]

[1]Bio Optics and Acoustics Laboratory, Departments of Creative IT Engineering and Electrical Engineering, Pohang University of Science and Technology (POSTECH), Pohang, 790-784, Republic of Korea; [2]School of Electrical and Electronic Engineering, Yonsei University, Seoul, 120-749, Republic of Korea; [3]School of Chemical and Biomedical Engineering, Nanyang Technological University, Singapore 637459.

ABSTRACT

Super-resolution microscopy has been increasingly important to delineate nanoscale biological structures or nanoparticles. With these increasing demands, several imaging modalities, including super-resolution fluorescence microscope (SRFM) and electron microscope (EM), have been developed and commercialized. These modalities achieve nanoscale resolution, however, SRFM cannot image without fluorescence, and sample preparation of EM is not suitable for biological specimens. To overcome those disadvantages, we have numerically studied the possibility of super-resolution photoacoustic microscopy (SR-PAM) based on near-field localization of light. Photoacoustic (PA) signal is generally acquired based on optical absorption contrast; thus it requires no agents or pre-processing for the samples. The lateral resolution of the conventional photoacoustic microscopy is limited to ~200 nm by diffraction limit, therefore reducing the lateral resolution is a major research impetus. Our approach to breaking resolution limit is to use laser pulses of extremely small spot size as a light source. In this research, we simulated the PA signal by constructing the three dimensional SR-PAM system environment using the k-Wave toolbox. As the light source, we simulated ultrashort light pulses using geometrical nanoaperture with near-field localization of surface plasmons. Through the PA simulation, we have successfully distinguish cuboids spaced 3 nm apart. In the near future, we will develop the SR-PAM and it will contribute to biomedical and material sciences.

Keywords: Biological imaging, nanoscale, optical imaging, sub-diffraction-limit imaging

1. INTRODUCTION

Super-resolution microscopy (SRM) technologies [1] overcome the diffraction limit of light [2] and enables the investigation of biological samples ranging from individual nano-sized organisms to whole cell organelles [3]. Super-resolution fluorescence microscopy (SRFM) [4] is a widely used technique for living specimens because it can distinguish specific cellular components using molecular-specific exogenous fluorescent agents. However, fluorescent materials are generally not preferred because they can degrade the effective resolution of SRFM [5] due to photobleaching and can damage biological samples [6]. Electron Microscopy (EM) is another available SRM technology. EM has obtained atomic resolution [7], but there are many practical limitations on actual samples. One of the biggest limitations is that the sample must be in a vacuum environment. Therefore, the sample must be fixed, sliced, and dehydrated for imaging. Also, EM systems are extremely expensive and costly to maintain.

Photoacoustic (PA) imaging is a hybrid biomedical imaging method for examining organelles to organs [8-12]. PA imaging follows two main principles. (1) the molecules convert the absorbed light into heat and then induce thermal-elastic expansion of the object to generate PA waves, and (2) detect and reconstruct the PA wave to form a PA image. The contrast of PA images depends on the optical absorption capacity of various endogenous molecules such as DNA / RNA, hemoglobin and melanin. Therefore, exogenous agents are not generally required to distinguish targets within the PA image. Recently, several works have shown that photoacoustic imaging (PAI) systems can image nanoscale biological samples [13-16]. All of these super-resolution PAI techniques overcome the diffraction limit, but there is still

Photons Plus Ultrasound: Imaging and Sensing 2018, edited by Alexander A. Oraevsky, Lihong V. Wang, Proc. of SPIE Vol. 10494, 104945T · © 2018 SPIE · CCC code: 1605-7422/18/$18 · doi: 10.1117/12.2289418

the resolution limit to investigate <10 nm size samples [17]. In order to overcome these limitations, recently super-resolution visible photoactivated atomic force microscopy (pAFM) has been developed [13]. The pAFM has achieved ~ 8 nm lateral resolution using a tip. Near-field scanning optical microscope (NSOM) [18] is another SRM system. NSOM achieves super-resolution of less than 50 nm using an optical fiber tip with a pore size of 50 nm or less, but requires a contrast agent because only fluorescence signals are detected in the sample. Applying the method similar to that of NSOM, super-resolution PAI can achieve <10 nm resolution without exogenous agents.

In this study, a three-dimensional simulation of a super-resolution photoacoustic microscope (SR-PAM) using a plasmon nanoaperture is presented. To overcome the diffraction limit of light, we used RSoft Photonics CAD to induce femtosecond laser pulses under the nano-aperture to confirm near-field localization of less than 10 nm [19]. Using the near-field localization generated, we simulated the PA image by implementing a three-dimensional SR-PAM system using the k-Wave toolbox in MATLAB [20]. The simulation results also show the possibility of describing nanoscale samples using the proposed SR-PAM system.

2. METHODS

2.1 Modeling and Simulation of Near-fields Distribution Induced by Ultrashort Light Pulses

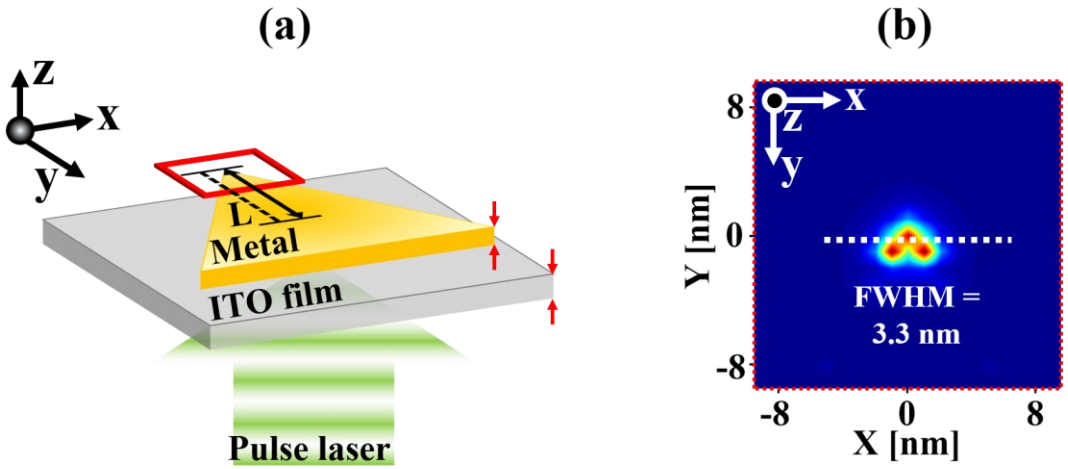

Figure 1. (a) Three-dimensional schematic of near-fields localization simulation. Metal nanoaperture on ITO film with a size of L = 150 nm. The widths of nanoaperture and ITO film set to 15 nm and 30 nm, respectively. Pulse laser irradiation perpendicular to the nanoaperture. (b) Closed-up image of enhanced near-field localization at a vertex of the nanoaperture from red box in panel a. Calculated full width at half maximum was 3.3 nm. ITO film, Indium tin oxide film.

We modeled a periodic triangular metal nanoaperture with a size of L = 150 nm and a period of Λ = 500 nm to induce an enhanced near-field localization (Fig. 1a). The size and period were chosen to avoid a plasmonic quadrupole and near-field inter-aperture coupling, otherwise the field enhancement of the metal aperture would be reduced and ultimately the resolution of the PA imaging would be reduced. The metal nanoaperture was set at 15-nm height and modeled with a 30-nm thick ITO layer. We used the femtosecond Gaussian pulse expressed in Eq. (1) to derive the local near field:

$$f(t) = \frac{1}{\sqrt{\pi}\tau} exp\left[-\left(\frac{t-t_d}{\tau}\right)^2\right] sin\left(\frac{2\pi c}{\lambda_0}t\right) \quad (1)$$

where, t_d and τ are the delay time and the pulse width, and c is the speed of light. The Gaussian pulse had a temporal full width at half maximum (FWHM) of 50 fs, a spectral line width of 50 nm, a center wavelength of λ_0 = 850 nm, and a normal incident to the nanoaperture array. The spot size of the pulse light was not defined because the pulse light

uniformly induced the entire nanoaperture structure. The incident pulsed light was polarized in the y-direction, and the center wavelength selected for PA imaging showed the resonance behavior of metal nanoaperture in the intensity spectrum. Based on the above mentioned values, a simulation of near-field localization in the metal nanoaperture was performed. Fig. 1(b) was the closed-up image of the red box in Fig. 1(a). This shows the near-field distribution formed at the vertex of the nanoaperture when the broad pulse laser is incident in the same direction as Fig. 1(a). To measure the size of the near-field, a profile was obtained along the white dashed line in Fig. 1(b) and Gaussian fitting was performed, and the full width at half maximum at that time was 3.3 nm. This simulated near-field was imported to the super-resolution PAI simulation as a light source.

2.2 Three-dimensional Photoacoustic Imaging Simulation using k-Wave Toolbox in MATLAB

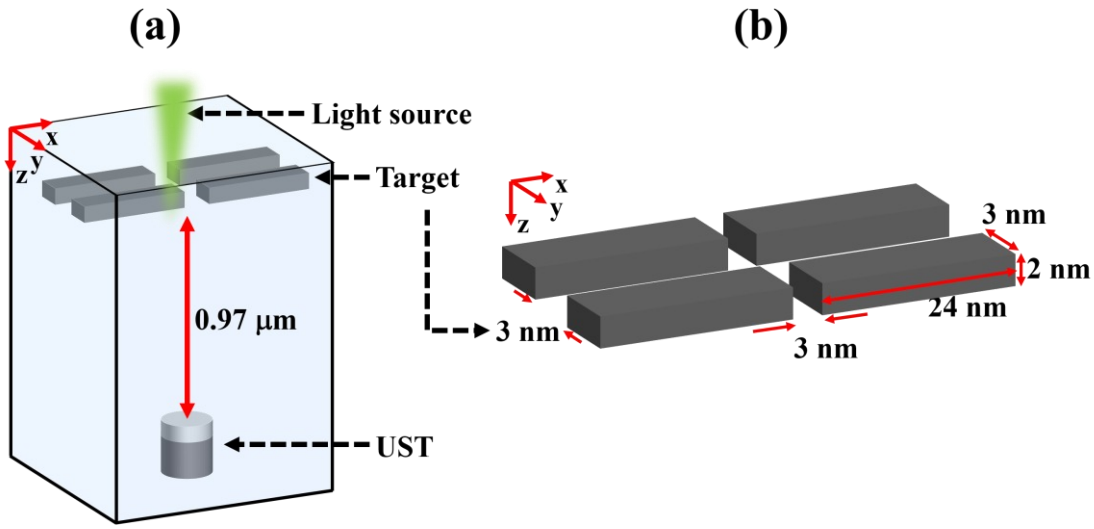

Figure 2. (a) Three-dimension simulation schematic of super-resolution photoacoustic imaging. (b) Closed-up image of the target. 4 cuboids were placed at 3 nm interval.

Using the k-Wave toolbox in MATALB, we simulated a super-resolution PA image using the enhanced near-field localization obtained in the previous step as the light source. The k-Wave toolbox was used only to generate PA data, and image processing and reconstruction were performed using the MATLAB general functions. We performed PA simulations on a graphics processing unit (GPU) to reduce computation time. The GPU was the NVIDIA TitanX with 3072 CUDA cores and 12GB of RAM. The simulation geometry was shown in Fig 2(a). The grid size was set to 120 (X-axis) × 120 (Y-axis) × 1000 (Z-axis) voxels and 1 nm / voxel. The single-element ultrasonic transducer was located 0.97 μm away from the center of the target in the Z-direction. The center frequency of the transducer was set at 1 GHz and had a bandwidth of 90%. Assume that the medium was water, acoustically homogeneous, and without loss. A target was used as the numerical phantom for the simulation. The phantom was made up of four cuboids, 24 nm (X-axis) × 3 nm (Y-size) × 2 nm (Z-size) in size (Fig. 2b). These four cuboids were arranged at intervals of 3 nm to confirm whether the proposed imaging system can distinguish adjacent cuboids.

3. RESULT AND DISCUSSION

The target consisting of four cuboids was excited using the light source generated by the previous simulation. In a three-dimensional environment, two B-scan images were acquired in planes A and B of Fig. 3(a), respectively. Because each cuboid was 3 nm apart from the other cuboids, we focused on whether the 3 nm was properly decomposed in the B-scan images by using the proposed SR-PAM system. In Fig. 3(b), it can be seen that the gap between the two cuboids was about 1.4 nm. This interval was the FWHM value calculated after Gaussian fitting in the line profile along the blue dashed line. Considering that the actual gap was 3 nm, it was expressed as about 2.1 times closer. In Fig 3(c), the gap between two cuboids was calculated in the same manner as in Fig. 3(b), and the value at this time was 2.0 nm. It was about 1.5 times closer than the actual spacing of 3 nm. This result was slightly improved compared to Fig. 3(b) because

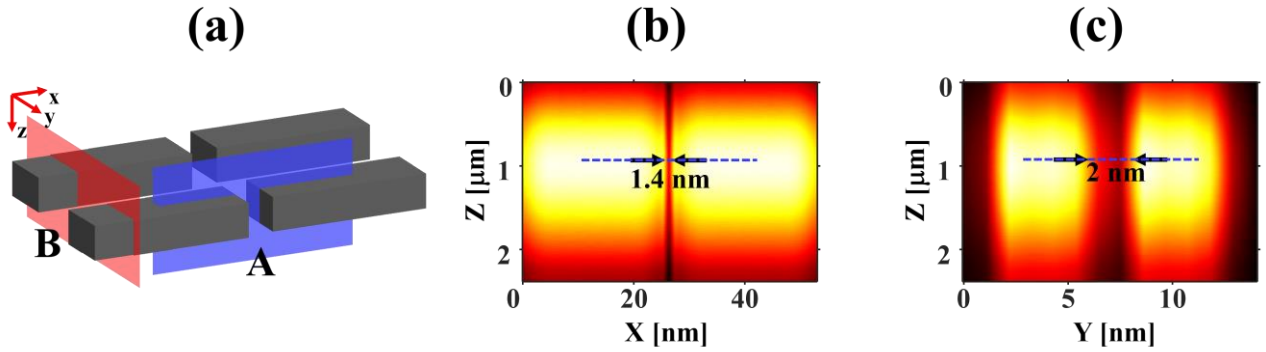

Figure 3. (a) Four cuboids target image with plane A and B. B-scan images along (b) the plane A and (c) the plane B.

the shape of the light source used in the simulation was a triangle rather than a complete sphere. Due to the nature of these light sources, different results were obtained depending on the scanning direction.

4. CONCLUSION

In this simulation study, we performed two simulations of an enhanced near-field localization and a super-resolution PAI system. The near-field showed about 3.3 nm spot size. In particular, we succeeded in distinguishing cuboids spaced 3 nm apart from each other, and we could confirm the results that vary depending on the scanning direction. Based on these results, we can conclude that this proposed system can be applied to various nanoscale biomedical applications in the future.

ACNOWLEDGEMENTS

This research was supported by grants from Consilience Creative program (IITP-2017-R0346-16-1007) of the MSIT (Ministry of Science and ICT) supervised by the IITP (Institute for Information & communications Technology Promotion), the Korea Health Technology R&D Project (HI15C1817) through the KHIDI (Korea Health Industry Development Institute) funded by the Ministry of Health & Welfare and the National Research Foundation of Korea (NRF) grant (No. 2011-0030075) of the MSIP (MSIT and Future Planning).

REFERENCES

[1] C. G. Galbraith, and J. A. Galbraith, “Super-resolution microscopy at a glance,” J Cell Sci, 124(10), 1607-1611 (2011).
[2] E. Abbe, “Beiträge zur Theorie des Mikroskops und der mikroskopischen Wahrnehmung,” Archiv für mikroskopische Anatomie, 9(1), 413-418 (1873).
[3] S. W. Hell, S. J. Sahl, M. Bates *et al.*, “The 2015 super-resolution microscopy roadmap,” Journal of Physics D: Applied Physics, 48(44), 443001 (2015).
[4] B. Huang, M. Bates, and X. Zhuang, “Super-resolution fluorescence microscopy,” Annual review of biochemistry, 78, 993-1016 (2009).
[5] H. Giloh, and J. W. Sedat, “Fluorescence microscopy: reduced photobleaching of rhodamine and fluorescein protein conjugates by n-propyl gallate,” Science, 217(4566), 1252-1255 (1982).
[6] Y. Inagaki, Y. Matsumoto, M. Ishii *et al.*, “Fluorescence imaging for a noninvasive in vivo toxicity-test using a transgenic silkworm expressing green fluorescent protein,” Scientific reports, 5, 11180 (2015).
[7] R. Erni, M. D. Rossell, C. Kisielowski *et al.*, “Atomic-resolution imaging with a sub-50-pm electron probe,” Physical review letters, 102(9), 096101 (2009).
[8] J. Kim, S. Park, Y. Jung *et al.*, “Programmable real-time clinical photoacoustic and ultrasound imaging system,” Scientific reports, 6, (2016).

[9] J. Kim, D. Lee, U. Jung *et al.*, "Photoacoustic imaging platforms for multimodal imaging," Ultrasonography, 34(2), 88 (2015).
[10] C. Kim, C. Favazza, and L. V. Wang, "In vivo photoacoustic tomography of chemicals: high-resolution functional and molecular optical imaging at new depths," Chemical Reviews, 110(5), 2756-82 (2010).
[11] C. Lee, S. Han, S. Kim *et al.*, "Combined photoacoustic and optical coherence tomography using a single near-infrared supercontinuum laser source," Applied optics, 52(9), 1824-1828 (2013).
[12] D. Lee, C. Lee, S. Kim *et al.*, "In vivo near infrared virtual intraoperative surgical photoacoustic optical coherence tomography," Scientific reports, 6, 35176 (2016).
[13] S. Lee, O. Kwon, M. Jeon *et al.*, "Super-resolution visible photoactivated atomic force microscopy," Light: Science & Applications, 6(11), e17080 (2017).
[14] A. Danielli, K. Maslov, A. Garcia-Uribe *et al.*, "Label-free photoacoustic nanoscopy," Journal of biomedical optics, 19(8), 086006-086006 (2014).
[15] J. Yao, L. Wang, C. Li *et al.*, "Photoimprint Photoacoustic Microscopy for Three-Dimensional Label-Free Subdiffraction Imaging," Physical Review Letters, 112(1), 014302 (2014).
[16] P. K. Upputuri, and M. Pramanik, "Microsphere-aided optical microscopy and its applications for super-resolution imaging," Optics Communications, (2017).
[17] H. P. Erickson, "Size and shape of protein molecules at the nanometer level determined by sedimentation, gel filtration, and electron microscopy," Biological procedures online, 11(1), 32 (2009).
[18] E. Betzig, A. Lewis, A. Harootunian *et al.*, "Near field scanning optical microscopy (NSOM): development and biophysical applications," Biophysical Journal, 49(1), 269-279 (1986).
[19] H. Lee, C. Kim, and D. Kim, "Sub-10 nm near-field localization by plasmonic metal nanoaperture arrays with ultrashort light pulses," Scientific reports, 5, (2015).
[20] B. E. Treeby, and B. T. Cox, "k-Wave: MATLAB toolbox for the simulation and reconstruction of photoacoustic wave fields," Journal of biomedical optics, 15(2), 021314-021314-12 (2010).